

# Measurements of Loudspeakers with a Laser Doppler Vibrometer and the Exponential Sine Sweep Excitation Technique

MARIA COSTANZA BELLINI, *AES Student Member*, LUCA COLLINI, ANGELO FARINA, *AES Fellow*,  
(mariacostanza.bellini@gmail.com) (luca.collini@unipr.it) (angelo.farina@unipr.it)

DANIEL PINARDI, AND KSENIIA RIABOVA  
(daniel.pinardi@unipr.it) (kseniia.riabova@unipr.it)

*University of Parma, Dept. of Engineering and Architecture, Parma, Italy*

This paper presents an experimental study of vibrations of the cone of loudspeakers. Measurements of the axial acceleration have been performed in hundreds of points on the surface of the cone employing a Laser Doppler Vibrometer and using the exponential sine sweep excitation signal. The recorded signal has been transformed into an impulse response by convolution with the matched inverse sweep signal. From the knowledge of the acceleration in each point of the radiating surface, the free field sound pressure in axis at 1 m distance has been computed.

The research focuses on obtaining results comparable to FEM simulations based only on the linear mechanical behavior of the loudspeaker cone and avoiding any acoustic interference. Moreover, comparing the laser measurements of many samples, the authors seek to evaluate the influence of known variations in the loudspeaker components or production process on the final performances of the device. Post-processing of experimental results is carried out employing a Matlab script, which also computes operational deflection shapes of the loudspeaker cone.

## 0 INTRODUCTION

The first acoustic applications of LDV—Laser Doppler Vibrometer—date back to 1978 with experiments conducted by Kinoshita on compression drivers [1] or with measurements made on condenser microphones by Behler in 2004 [2]. First LDV measurements on loudspeakers have been done by Moreno in 1991 [3] while a variety of methods are found in the quantitative measure of vibrations for acoustic application, e.g., [4–9].

Many different combinations of signal and sensors can be applied and have been tried in the past but it must be said that methods for LDV measurement developed before 2000 could not benefit of the exponential sine sweep technique, presented by Farina at the 108<sup>th</sup> AES Convention [10], while several recent studies have been conducted by Klippel from 2008 until now employing a triangulation laser and chirp signal [11].

The system presented in this article is based on a novel combination of test signal and sensor and consists in a LDV scanning system paired with the exponential swept-sine test signal. In this way, the sensitivity (in particular at higher frequencies) of LDV has been coupled with the high S/N ratio and robustness to uncorrelated noise provided by ESS technique.

The purpose of the research described below is not to demonstrate that acoustic measurement with microphones in an anechoic room can be substituted by an LDV system, but provides a method for mechanical measurement of cone vibrations and vibrational mode analysis to determine the variety of factors that might negatively influence the performance of this device. Modes of vibrations that occur when a loudspeaker is operating strongly influence the radiated sound field and, furthermore, the actual sound perceived by listeners. The acoustical frequency response is sensitive to even minor variations in the materials and assembly of the device. Hence, it is important to develop a procedure for the sensitivity analysis of the loudspeaker response with respect to possible modifications in the production process.

Moreover, the method developed and explained here can be used to acquire quantitative data about mechanical behavior of the loudspeaker, information that is the base for other and more accurate studies, based on FEM simulation of the cone vibrations where acoustic field is not computed.

The research was conducted for a typical loudspeaker used in a car sound system: a “door woofer” designed to operate between 200 Hz and 5 kHz; indeed in this research the focus was in the frequency range from 500 Hz

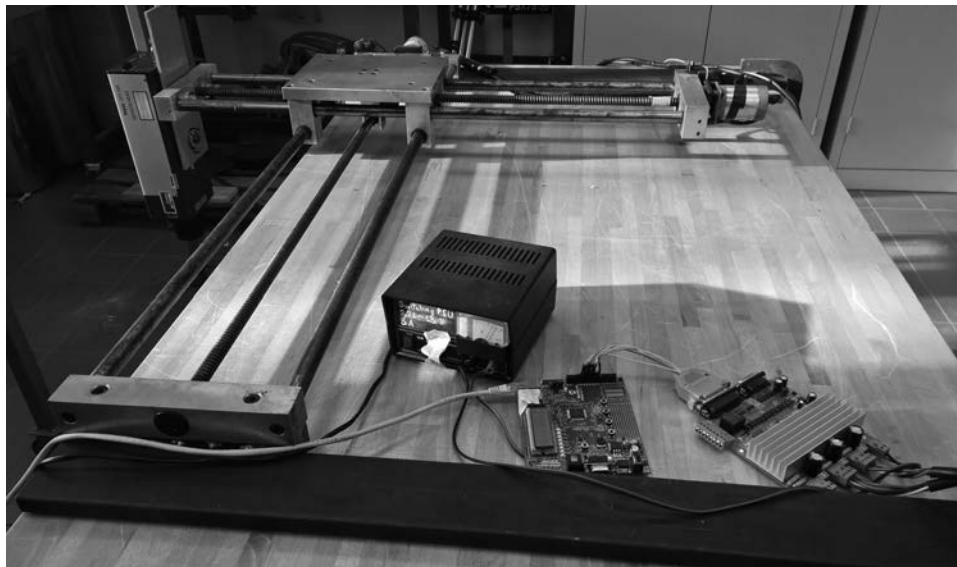


Fig. 1. Positioning system

to 10 kHz because the low-frequency pistonic behavior is of no interest, and on the other side it is useful to evaluate parasitic vibrations affecting higher harmonics of the base signal.

Besides the experimental analysis executed by means of the laser vibrometer, a numerical model of the loudspeaker was developed employing a finite element software that will be described in a subsequent paper. These activities combined allowed us to get an insight on specific properties of the loudspeaker and its components. The results of the extrapolated SPL curve, computed according to the simplified theory presented by Klippel in [12], are presented in comparison with physical measurements of the radiated acoustic pressure carried out in an anechoic room.

## 1 EXPERIMENTAL MEASUREMENTS

The experimental measurements reported here were carried out in the laboratory of the Department of Engineering and Architecture at the University of Parma, Italy. The experimental setup was composed of a Laser Doppler Vibrometer accompanied by a two-axes positioning system with step motors, a power amplifier, and a sound card all controlled via a laptop computer. The software controlling the measurement procedure, data acquisition, and further elaboration of results was coded in Matlab.

### 1.1 Experimental Setup

The mechanical part of the measurement chain consisted of the laser sensor head Polytec OFV 505 mounted on a frame connected to two independent perpendicular axes in the horizontal plane. Each of the axes has a step motor that enables a displacement of the laser head along the assigned axis; both are controlled by an electronic board connected via Ethernet to the laptop (Fig. 1).

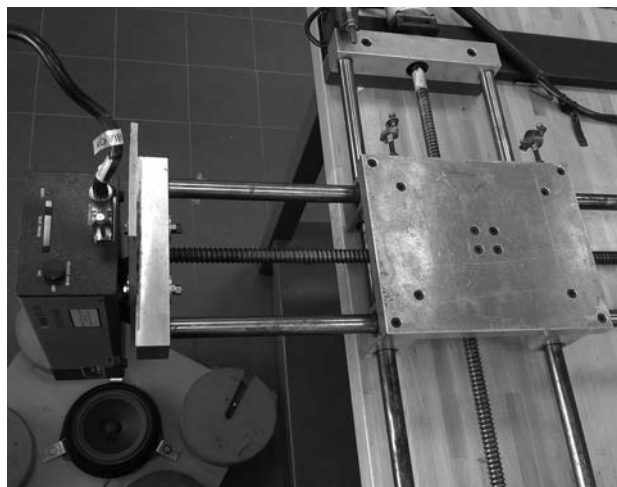


Fig. 2. Loudspeaker support under sensor head

In this way the laser can be relocated precisely by providing the Cartesian coordinates  $x$  and  $y$  through a Matlab interface. The vertical ( $z$ ) coordinate of the sensor head, thus, remained constant. The loudspeaker under test was positioned on the floor under the laser, fixed in a rigid wooden frame insulated in a way that ensured the absence of unwanted vibrations of other elements of the setup besides the speaker itself, as shown in Fig. 2.

As the vertical coordinate of the sensor head was kept constant while the loudspeaker profile is not flat (it changes along the radius), the software provided to activate the autofocus function every time needed, depending on the scanning grid.

The sound card was connected to a laptop and a power amplifier and the latter to the loudspeaker—these devices combined formed the output branch of the system. The laser sensor head, the vibrometer controller, and the preamplifier of the sound card formed the input branch of the system (Fig. 3).



Fig. 3. Control system

The voltage of the signal sent to the speaker was kept constant at 0.500 Vrms, making sure that the tests were reproducible.

**1.1.1 Grid Generation**

Based on the input parameters, i.e., the working diameter of the loudspeaker and the desired number of circumferences on the discretized surface, the program generates a two-dimensional grid of equally spaced points starting from the center of the loudspeaker.

In order to “catch” the complicated shapes of vibration modes at high frequencies it is essential to have a

sufficient number of points representing the radiating surface (radiator), which in turn leads to the discussion on resolution versus measurement time. It should be mentioned that for a very detailed grid a test could last more than 13 hours and since, in the frame of this research, it was foreseen to investigate a significant number of samples, the problem of grid optimization became critical.

Therefore, several tests with different grids were carried out on the same sample in order to find the minimal necessary number of points that could provide a satisfactory resolution. In Fig. 4 the comparison between three different types of grids is presented, both as Accumulated

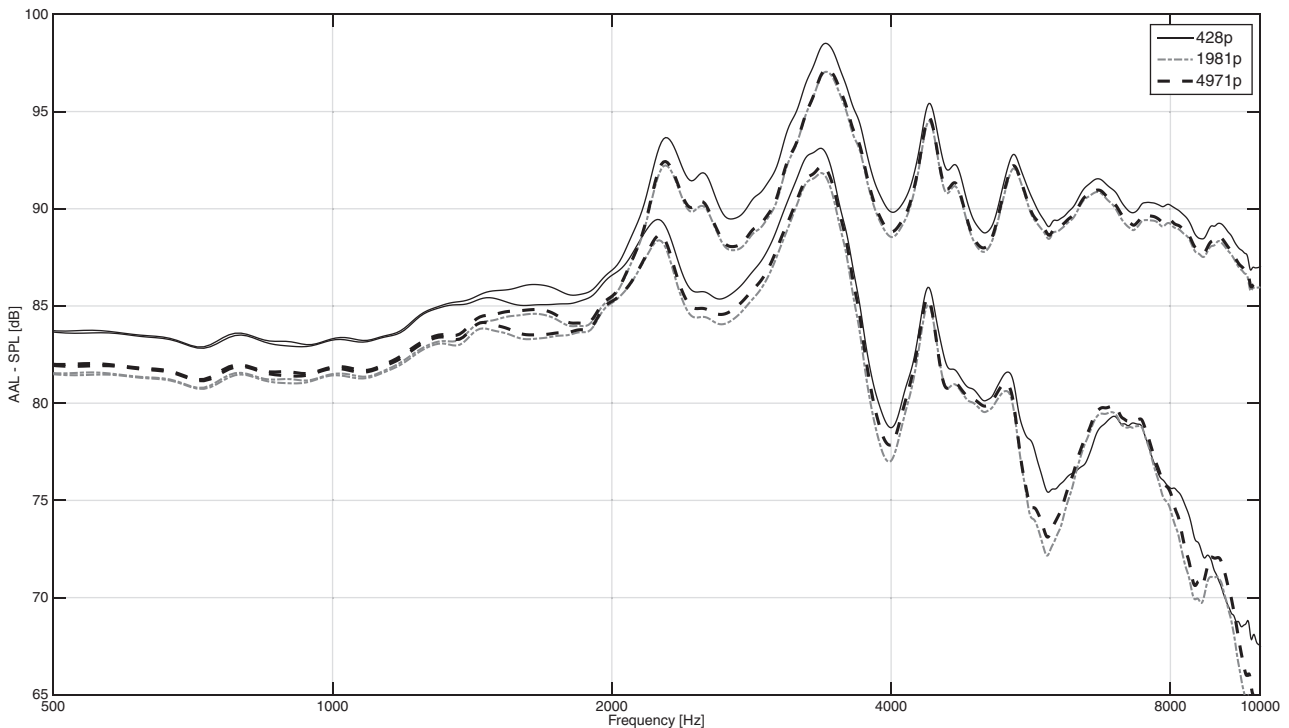


Fig. 4. Grid comparison

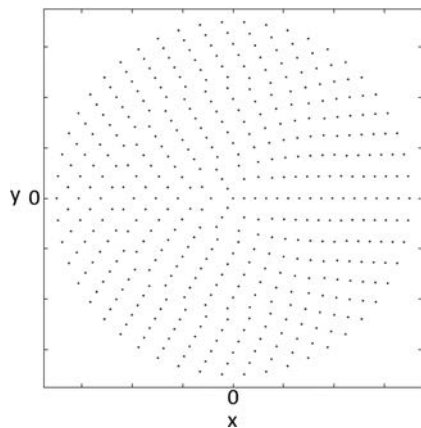


Fig. 5. Measurement grid (428 points)

Acceleration Level (AAL) and extrapolated Sound Pressure Level (SPL) curves:

- 16 concentric circles for an amount of 428 points. Measurement time: 1h40’.
- 35 concentric circles for an amount of 1981 points. Measurement time: 4h.
- 70 concentric circles for an amount of 4901 points. Measurement time: 13h.

It is important to underline that grids are generated in a way to maintain constant the density of points, so that the spatial resolution is the same over the radiating surface.

It is noticeable that the results obtained with 1981 and 4901 points are almost coincident; the one with 428 points leads a not significant level offset, always equal or lower than 2 dB, but all peaks of the curves correspond up to 8 kHz. Only a small peak on the descending slope at 9 kHz is lost with 428 points. For these reasons the optimal grid is identified in the first one (Fig. 5), kept unchanged for all the tested loudspeakers.

The surface of the speaker from the point of view of the laser is presented as a 2D plane since the z coordinate is not taking part in the measurement itself; however, the profile of the surface was considered afterwards in the calculation of the radiated sound pressure.

### 1.2 Excitation and Acquisition of Vibrations

The concept of the experiment is to excite a loudspeaker with an exponential sine sweep signal and to record the output signal represented by the vibration response of the radiating surface (paper cone, dust cap, and rubber surround). A description of the procedure and the mathematical background of the exponential sine sweep measurement technique were introduced in [10].

When computing the impulse response (IR) of a system, there are typically two problems. The first one is related to the noise that enters the system and becomes a part of the output signal; the second one instead is caused by nonlinearities and distortion inherent to the transducers and system itself (no real world system is really linear, nor time invariant). The first issue is normally overcome by

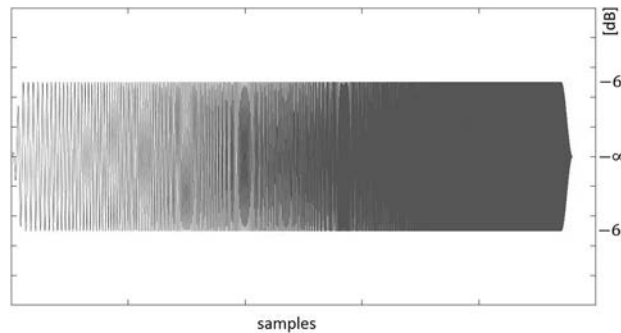


Fig. 6. Sweep signal

averaging the output signal, but this is possible only if the system is really time-invariant, while the second one is not so trivial to solve. One of the main advantages of the linear deconvolution in the time domain is the separation of non linear distortion products that appear in the IR of the system.

The formula for generating an exponential sweep signal is presented by Eq. (1) [10].

$$x(t) = \sin \left[ \frac{2 \cdot \pi \cdot f_1 \cdot T}{\ln \left( \frac{f_2}{f_1} \right)} \cdot \left( e^{\frac{t}{T} \cdot \ln \left( \frac{f_2}{f_1} \right)} - 1 \right) \right] \quad (1)$$

In Eq. (1)  $f_1$  is the starting frequency,  $f_2$  is the end frequency of the sweep,  $T$  is the total duration in seconds,  $t$  is current time.

The choice of  $f_1$ ,  $f_2$ , and  $T$  is not completely free as an exponential sine sweep is optimal only if it is “synchronized” according to Novak’s theory [13], which means that whenever the instantaneous frequency becomes a power-of-two times the starting frequency (that is, at every octave), the signal should be zero and with positive derivative (a sine starting up). This ensures that all the multiple impulse responses obtained due to harmonic distortions will be phase-synchronized.

The synchronization condition is ensured by imposing this constraint:

$$\frac{T \cdot f_1}{\ln \left[ \frac{f_2}{f_1} \right]} \in \Re \quad (2)$$

which usually is satisfied by adjusting the duration  $T$ .

A further refinement of the method employs half-Hann windows at the start and end of the sweep signal for avoiding “border effects” [14].

The synchronized sweep signal is generated in Adobe Audition using the Aurora plug-in [15] on a frequency range quite larger than the one to be measured, for ensuring that the signal inside the operational frequency range is stable. An inverse filter  $f(t)$  is automatically generated and stored for further convolution with the recorded response signal in order to obtain the IR of the system (see Fig. 6–7 for the signals).

The convolution of the sweep signal with the inverse filter  $f(t)$  results in a delayed, band-limited Dirac’s delta function. If instead the recorded signal from the Laser Doppler

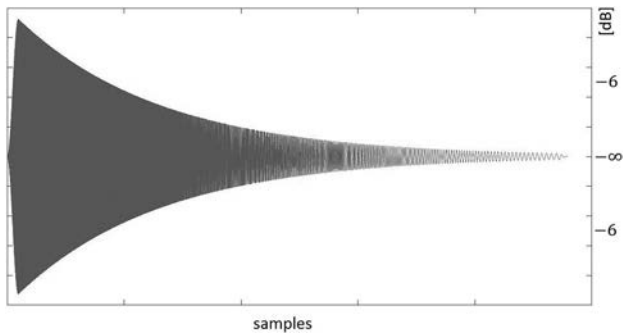


Fig. 7. Inverse sweep signal

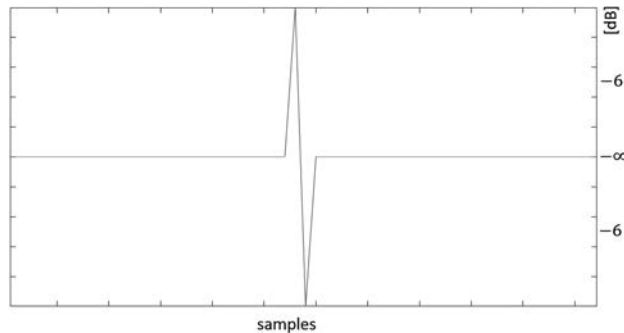


Fig. 10. Unit doublet signal

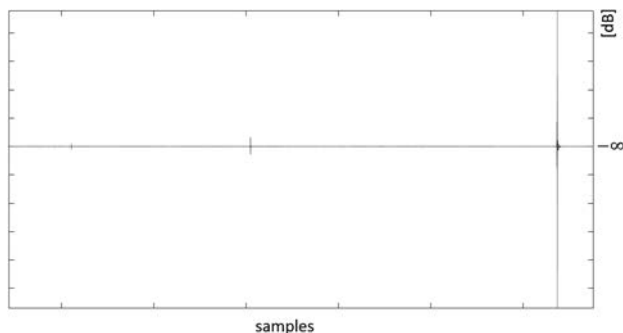


Fig. 8. Complete response with not-linear responses

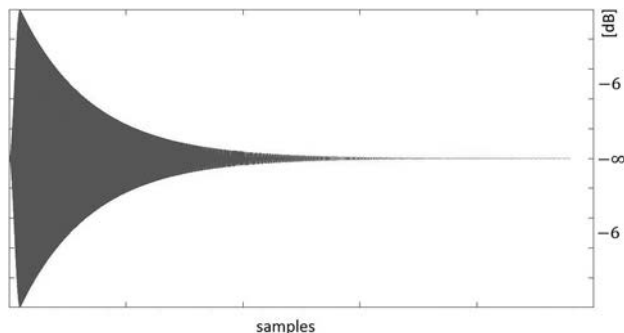


Fig. 11. Differentiated inverse sweep  $f'(t)$

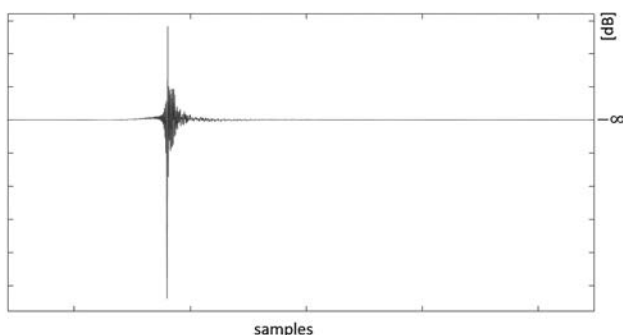


Fig. 9. Linear windowed IR

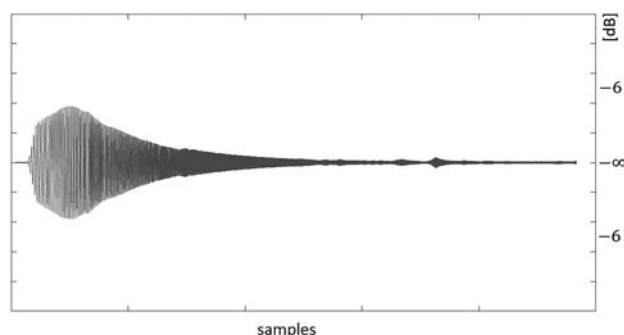


Fig. 12. Recorded sweep

velocimeter is convolved with the inverse sweep (Eq. (3)), the result is the impulse response of the system  $h(t)$ :

$$h(t) = y(t) \otimes f(t) \tag{3}$$

If the system is not linear (in practice, always), the results are not just the linear impulse response  $h(t)$ , but also the not-linear impulse responses are obtained, corresponding to the various harmonics of the input signal. These not-linear products, indeed, do not contaminate the linear response, as they are occurring at anticipatory times, before the linear impulse response  $h(t)$  (Fig. 8). Hence, a simple windowing in time domain removes completely these not-linear products (Fig. 9).

In the continuation of this research these harmonic distortion responses will not be discarded but analyzed, as the not-linear behavior of the loudspeaker vibrations is also a powerful indicator of possible manufacturing problems.

The controller of the laser, a Polytec OFV-5000, outputs an analog electrical signal proportional to the velocity, but for acoustical analysis it is better to measure acceleration,

hence a differentiation operation is needed. To provide this result, the inverse sweep signal  $f(t)$  was differentiated. This is obtained very simply by convolving  $f(t)$  with the “unit doublet signal” (Fig. 10), which in practice is a signal of a certain number of samples, all equal to zero, except for two consecutive, having values  $+1$  and  $-1$ .

The convolution between a velocity signal and the unit doublet produces an acceleration signal. Due to the linear property of convolution, it has been possible to convolve the inverse sweep with the unit doublet, obtaining a differentiated inverse filter  $f'(t)$  (Fig. 11), packing the two operations into one and saving computation time.

The sweep signal was sent to the loudspeaker through the sound card and the power amplifier causing its vibrations, while the laser vibrometer sends the velocity signal back to the sound card. In this way the output signals were recorded into wav files (Fig. 12).

After the output signal of each point was convolved with the inverse filter and properly windowed (Fig. 9), a matrix of IRs was formed and a Fast Fourier Transform (FFT)

spectrum was calculated for each measurement point. Further elaboration of the data allowed for the computation of the complex spectrum of acceleration correctly calibrated in  $\text{ms}^{-2}$ . This makes it possible to use these results for the calculation of quantities integrated over the whole radiating surface, such as the total accumulated acceleration level (AAL) and the total sound pressure level (SPL), evaluated in a reference point (at 1 m distance, on axis). In this way it is possible to compare the results of laser vibrometry with anechoic acoustical measurements executed with a standard pressure microphone.

### 1.3 Calibration and Validation of Measurement Chain

In many cases, when performing vibration measurements, the goal is to obtain the natural frequencies of the system and the amplitude of vibrations itself is not the point of interest. In the present study, on the contrary, the amplitude has to be known accurately since this value is further processed into SPL and AAL calculations. That is why the complete experimental setup needs to be calibrated, which revealed to be not trivial.

The first step of calibration is to measure vibrations of known amplitude. For this purpose the loudspeaker was replaced with an accelerometer calibration exciter Bruel&Kjær 4294 and the vibration of its aluminium piston was measured via the laser vibrometer. The most important detail that must be remembered is that it vibrates at 159.2 Hz, with a RMS velocity level in dB (re to 1 nm/s) and a RMS acceleration level in dB (re to  $1 \mu\text{m/s}^2$ ) that are both equal to 140 dB: only at this particular frequency, where  $\omega = 1000 \text{ rad/s}$ , the decibel scales of velocity and acceleration produce the same value thanks to the choice of their reference values. This is important in our case, as we are using a velocity transducer for measuring acceleration levels. The input scale factor is adjusted, so that the calibrator's signal is read as a velocity level of 140 dB.

The second step is to excite the loudspeaker with a steady sinusoidal signal at the same frequency of 159.2 Hz and with the standard amplitude of  $0.5 V_{\text{RMS}}$ , and to record the response in the central reference point. Now the real velocity and acceleration level at this frequency can be measured (the value is typically around 156 dB).

The third and final step of the calibration procedure is to send a sweep signal to the loudspeaker, again with a constant voltage of  $0.5 V_{\text{rms}}$ , with a frequency range embracing the calibration frequency of 159.2 Hz and recording the response at the same reference central point. Then the recorded signal is convolved with the inverse sweep, keeping a constant rescaling gain (typically  $-60 \text{ dB}$ ), to compute the acceleration IR and get the acceleration spectrum by means of an FFT (see Fig. 13 for a chart of the magnitude of the acceleration spectrum in dB re to  $1 \mu\text{m/s}^2$ ).

The difference between the known value of acceleration at 159.2 Hz measured in Step 2 (for example, 156 dB) and the value appearing on the chart of the acceleration spectrum at the same frequency (for example 66 dB) defines the additional gain to be added to the results for getting

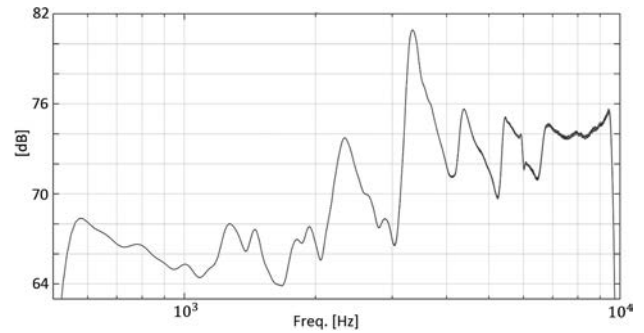


Fig. 13. Stability of measurement chain

calibrated acceleration levels. With the numbers provided as an example, this is an additional gain of  $156 - 66 = 90 \text{ dB}$ . This gain is to be applied to rescale all the experimental FRFs to calculate true acceleration levels. After this delicate calibration phase is completed, the measurements can be conducted safely, keeping the same settings (voltage, sweep signal, inverse filter, and FFT size) as used in the calibration.

In order to compare laser and microphone measurements, another factor has to be taken into account: the voltage applied to the loudspeaker by the power amplifier. If the loudspeaker is measured in the anechoic room at a different voltage, the SPL computed from the laser acceleration measurements has to be adjusted by a further offset calculated as  $20 \cdot \log\left(\frac{V_{\text{anechoic}}}{V_{\text{laser}}}\right)$ . In our case the loudspeaker has been measured in the anechoic room at 2 V and with the laser at 0.5 V, so the offset to be applied resulted to be  $+12 \text{ dB}$ .

To ensure a correct behavior of the measurement chain, some preliminary tests have been conducted. For the thermal stability check, the central point of the loudspeaker has been excited and measured consecutively 100 times: the result is shown in Fig. 13, where all the FFTs are superimposed. Apart from a negligible difference at high frequency (over 7 kHz the curves spread by less than 0.5 dB) the system is not affected by any shift due to loudspeaker temperature, which changed significantly, approximately by  $20^\circ\text{C}$ , during repeated operation.

In addition the complete test has been repeated several times over consecutive days at different times (morning, evening) with different room temperatures between  $15 \div 25^\circ\text{C}$  and no variations have been observed.

For the repeatability check, four measures have been done sequentially in a day; each time, the base has been removed from under the laser, the loudspeaker itself has been disconnected and removed from the base, then mounted, connected, and positioned with a new centering (that is done manually). Results are presented in Fig. 14; AAL curves are almost superimposed, and also SPL curves are coincident under 4 kHz, then they spread slightly, but remaining in a band of error equal or lower than 2 dB.

The linearity of the measurement chain has been tested too, with different combinations of amplifier voltage and laser sensitivity in order to determine the optimum balance between loudspeaker stimulation and S/N ratio and to avoid clipping.

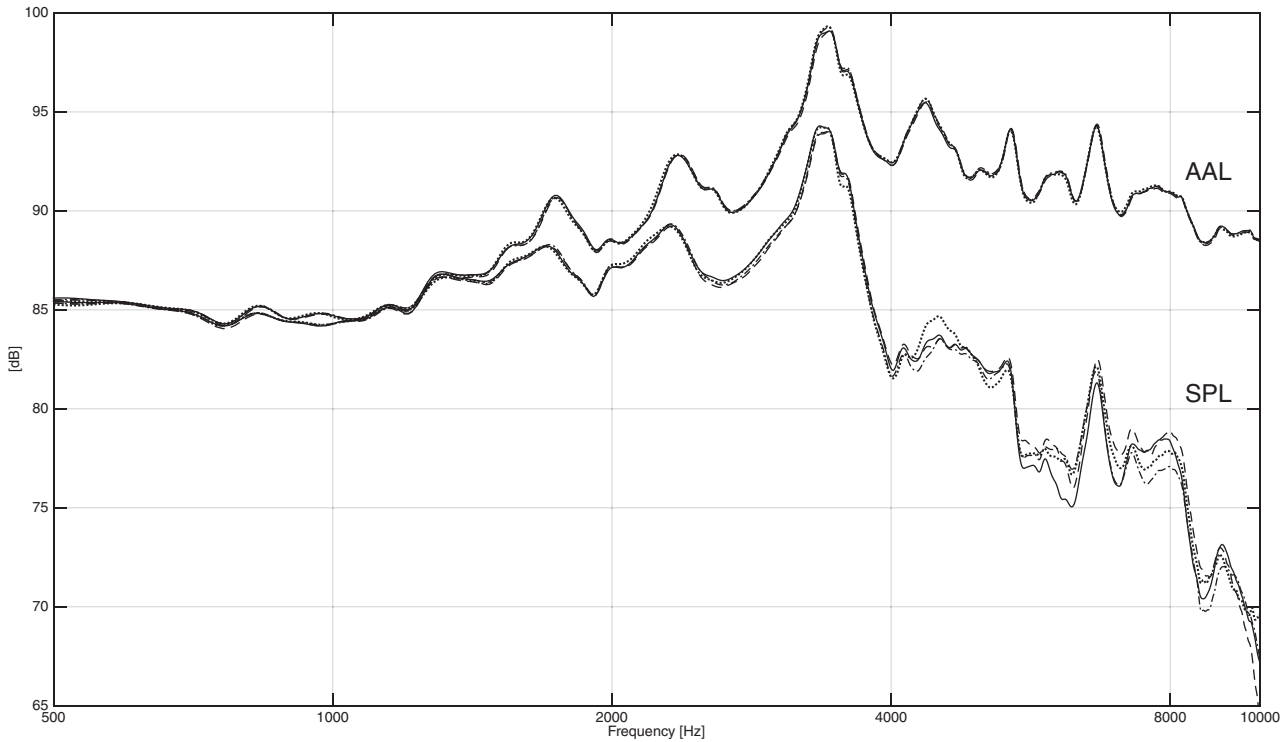


Fig. 14. Repeatability of measurement

Also, the mechanical cross-talk between loudspeaker, loudspeaker support, and sensor head has been verified. Any vibrations that are not correlated to the loudspeaker (for example the movement of positioning system for laser or low frequency vibrations of the floor for the support) are attenuated by more than 60 dB when convolution of recorded signal with inverse filter is performed; but this is not true if laser or support vibrations are induced by the loudspeaker itself and transmitted by support, floor, and table. In order to verify this unpleasant behavior is not affecting the system, two accelerometers have been placed on the loudspeaker support and on the laser sensor head. After calibration, a sweep signal has been sent to the loudspeaker and signals from laser and accelerometers have been recorded synchronously. Accelerometer signals have been convolved with a not differentiated inverse filter (they actually already measure acceleration), the laser signal has been convolved with the differentiated inverse filter, and their spectrums have been computed for comparison (Fig. 15).

In all the frequency range of interest the level of laser signal is always at least 33.5 dB above the vibration level measured on support or sensor head, meaning that the effects of the mechanical cross-talk are negligible.

### 1.4 AAL and SPL Computation

In order to validate the measurement method it has been necessary to compare the experimental vibrometric measurements with acoustical tests carried out in an anechoic room. For this reason the sound pressure level (SPL) curve has to be computed at the reference position (1 m distance, on axis).

The sound pressure level is defined by the Eq. (4) ( $p_0$  indicates the reference sound pressure).

$$SPL(f, \vec{r}_a) = 20 \log \left( \frac{|p(f, \vec{r}_a)|}{p_0} \right) \text{ dB}, \quad (4)$$

In Eq. (4) the average sound pressure is obtained from the Rayleigh integral (Eq. (5)), which is the approximation of Kirchhoff–Helmholtz formula [12] for sound radiation.

$$p(f, \vec{r}_a) = \frac{\rho_0}{2\pi} \int_{S_c} \frac{a(f, \vec{r}_c)}{|\vec{r}_a - \vec{r}_c|} e^{-jk|\vec{r}_a - \vec{r}_c|} dS_c, \quad (5)$$

In Eq. (5)  $\rho_0$  is the density of air,  $a$  is acceleration of a point with position  $r_c$  on a radiating surface  $S_c$ ,  $r_a$  indicates the point in which the pressure is calculated,  $f$  is frequency in Hz,  $j$  is the imaginary unit,  $k$  is the wave number defined as  $2\pi f/c$  ( $c$  is the speed of sound in air). In order to compare laser and anechoic measurements, the SPL curve has been computed at the reference anechoic measurement point, in axis with the loudspeaker at a distance of 1 m from the dust cup.

It is well known that the approximation adopted leads to a loss of accuracy that could be prevented by application of a more complex (and out of interest in this research) BEM calculation, but it must be remembered that the SPL comparison is needed only to validate the measurement system and not to create an alternative to the microphone for loudspeaker testing.

To compare the results of vibrational measurement of loudspeakers with the results of finite element simulations, another curve, AAL—accumulated acceleration level—has been computed. It indicates the total mechanical energy of vibration on the radiating surface. The values of AAL and

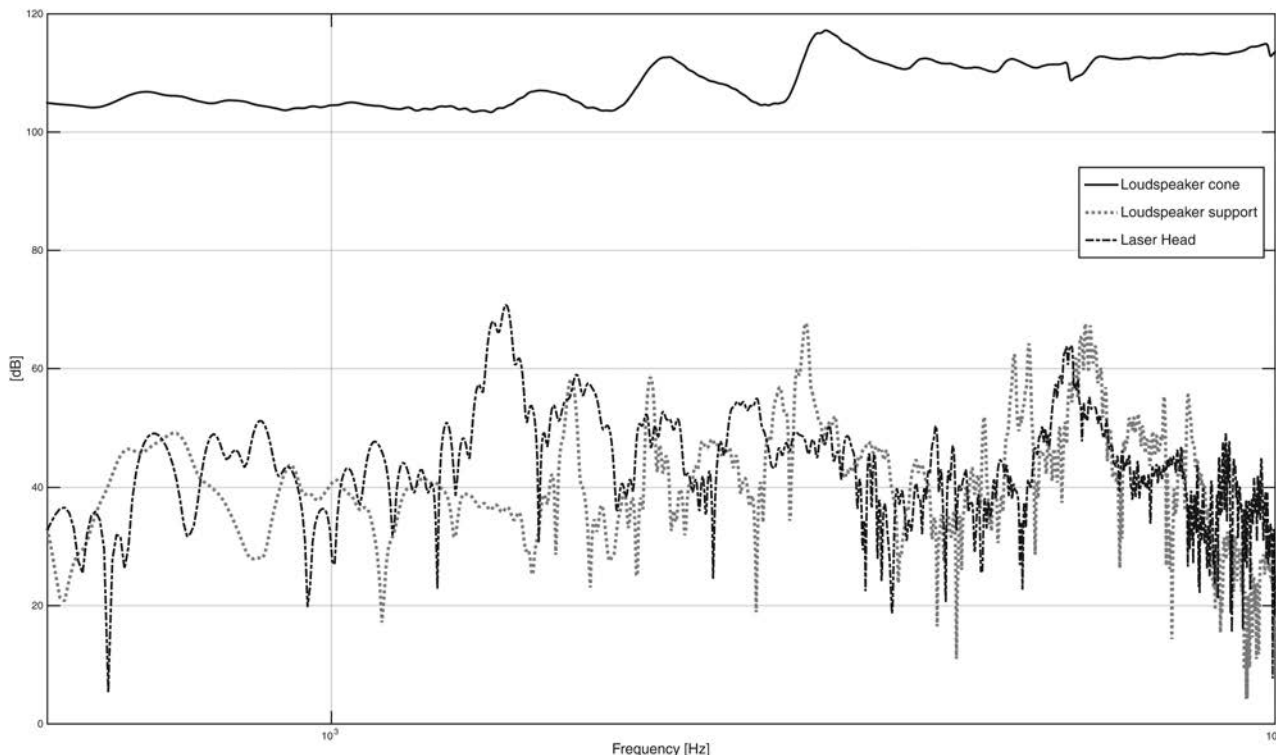


Fig. 15. Mechanical cross-talk check

SPL coincide on the range below the break-up frequency when the loudspeaker is vibrating in the so-called piston mode and there is no acoustic cancellation effect due to wave interference.

The accumulated acceleration level is computed from Eq. (6).

$$AAL(f, \vec{r}_a) = 20 \log \left( \frac{p_{aa}(f, \vec{r}_a)}{p_0} \right) \text{ dB}, \tag{6}$$

The accumulated acceleration  $p_{aa}$  in Eq. (5) is represented by the integral sum in form of Eq. (7).

$$p_{aa}(f, \vec{r}_a) = \frac{\rho_0}{2\pi} \int_{S_c} \frac{|a(f, \vec{r}_c)|}{|\vec{r}_a - \vec{r}_c|} dS_c, \tag{7}$$

As shown above, the acceleration is now taken in module, and this means that the exponential term that defines the phase is always equal to 1, neglecting interference of the waves radiated by different points of the vibrating surface.

In both Eqs. (4) and (6) it is necessary to divide the value of sound pressure and accumulated acceleration, correspondingly, by the square root of two, for converting the results to RMS values.

In Eqs. (5) and (7) it is also necessary to compute the term  $|\vec{r}_a - \vec{r}_c|$ , that is the distance between the point of radiation and the point where SPL is calculated. But, as mentioned before, the matrix of measurement points is associated only to the X,Y coordinates of each point, and information about the Z coordinate has to be estimated by the knowledge of the loudspeaker profile, which is shown in Fig. 16.



Fig. 16. Loudspeaker profile points

For each point, the value of Z is obtained interpolating the discretized profile of Fig. 12, in correspondence of the distance of the point from the loudspeaker axis.

The spectrum of accelerations  $a(f,rc)$  is represented by a complex number at each frequency for each point of the grid. In addition to that, the area of the surface associated with each point of the grid,  $dS_c$ , has been calculated: they are required when the integrals of Eqs. (5) and (7) are calculated numerically.

## 2 RESULTS AND DISCUSSION

The results are reported in terms of AAL and SPL curves and also as operational deflection shapes of loudspeaker vibrations at selected frequencies, corresponding to peaks or valleys in the curves.

### 2.1 AAL and SPL Curves

The resulting plots of AAL and SPL of a woofer that operates according to the manufacturer’s specifications are shown in Fig. 17. It is evident that the two curves coincide up to the break-up frequency, which proves that below it the



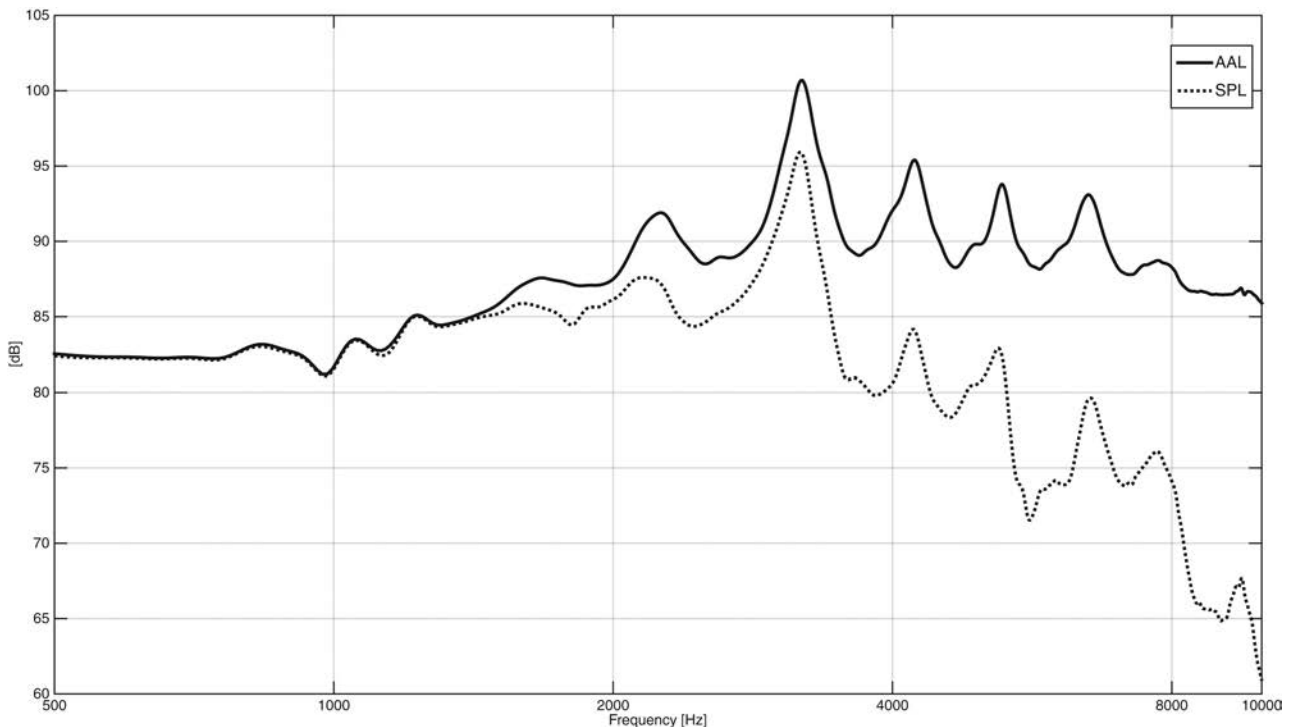


Fig. 17. AAL and SPL curves

loudspeaker is moving as a piston (rigid body mode) and there are no anti-phase components present in the sound pressure.

Once the curves split, the AAL always remains larger than SPL, since it represents the absolute value of vibrational energy while SPL takes into account the partial cancellation of the total radiated sound pressure caused by the anti-phase components. However, the frequencies indicating peaks and valleys in AAL and SPL curves remain the same.

As mentioned before, the absolute calibration of the laser vibrometry needs to be validated throughout comparison with the “true” SPL directly measured by a microphone inside an anechoic room. These tests were carried out in the anechoic room of the research laboratory of ASK Industries in Monte San Vito (AN), Italy. Comparison of the curves obtained with the two different approaches is presented in Fig. 18. At high frequencies the difference in the magnitude of amplitudes is related to Rayleigh approximation, at low frequencies instead it is related to the contribution of standardized wooden baffle where the loudspeaker is mounted on for anechoic measurement. Despite these facts, the calculation based on laser results managed to “catch” most of the significant peaks of the SPL/AAL, and with absolute values in dB, which were judged “close enough” for confirming the system calibration, proving that measurements with the laser vibrometer are suitable for studying the behavior of loudspeakers.

## 2.2 Operational Deflection Shapes

In addition, the modal shapes at the peak frequencies have been reconstructed. They provide important information about the behavior and quality of loudspeakers, presence

of defects (i.e., rocking mode), and further data for finite elements analysis validation.

Positive peaks of the AAL curve indicate the most energetic (i.e., “resonant”) vibration modes and, in reality, the smoother the response curves are, the better the sound quality of a loudspeaker is. Negative peaks of the SPL curve represent the condition of low efficiency for a loudspeaker, with little energy radiated. Visualization of vibration modes corresponding to the peaks and valleys (so-called operational deflection shapes) was carried out in Matlab and the script developed allowed even to emulate in a video the 3D response of a loudspeaker to the sweep excitation. In Fig. 19 the operational deflection shapes (ODS) of a woofer sample at the five most important AAL positive peaks are illustrated in 3D view: Fig. (19a) 2250 Hz, Fig. (19b) 3188 Hz, Fig. (19c) 4219 Hz, Fig. (19d) 5250 Hz, and Fig. (19e) 6516 Hz. The “piston” mode can be observed in Fig. 19f, and can be computed in the same way of ODS for all frequencies before break-up.

At higher frequencies the increase of the number of circumferences in the modal shape can be witnessed.

Overall the modes extracted from the vibrometric experiments correlate well with the results on the loudspeaker modal shapes previously reported in other scientific publications, e.g., in [16].

## 2.3 Analysis of Factors Influencing the Loudspeaker Vibrations

The acoustic response of the loudspeaker, and thus, its sound quality, can be significantly influenced by conditions of production process, slight changes in materials or variations of dimensions and characteristics of components even if within the range of tolerances.

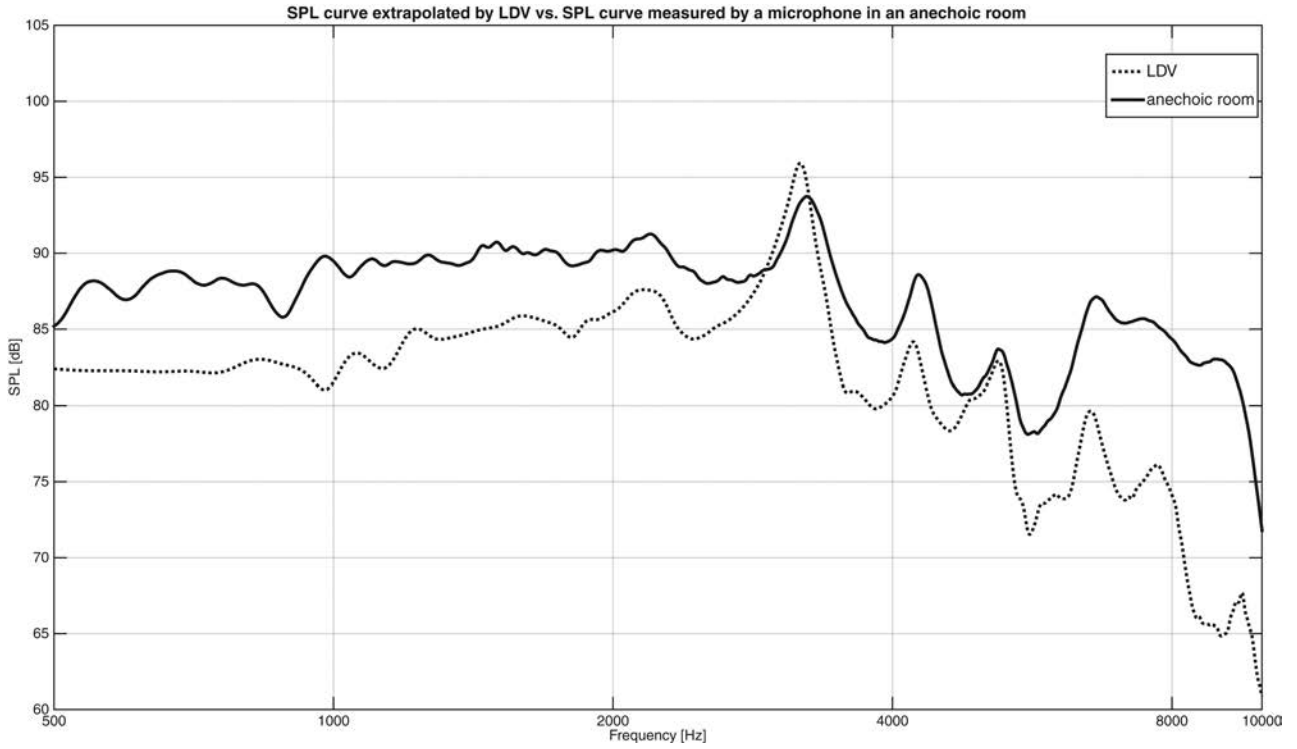


Fig. 18. SPL comparison between laser and anechoic measurement

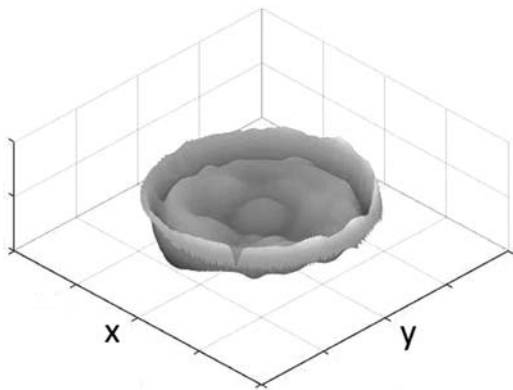


Fig. 19a. 2250 Hz

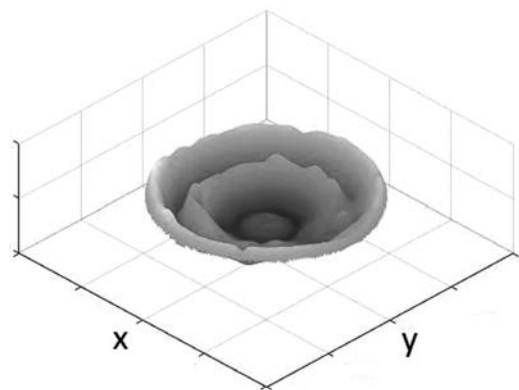


Fig. 19c. 4219 Hz

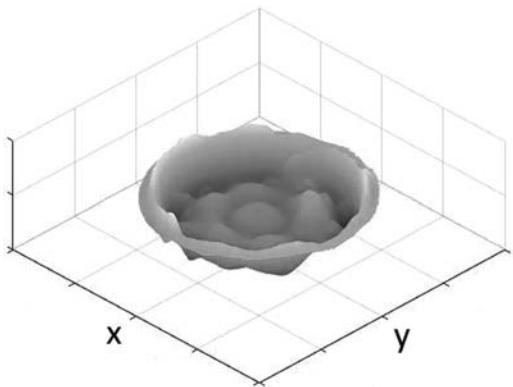


Fig. 19b. 3188 Hz

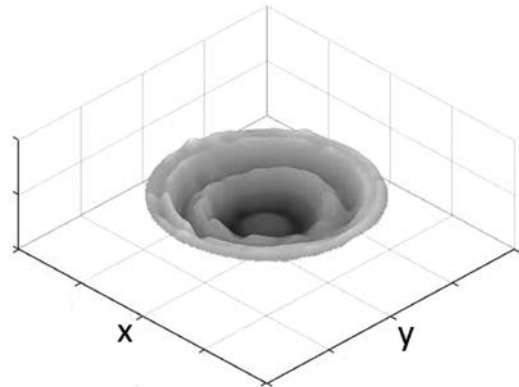


Fig. 19d. 5250 Hz

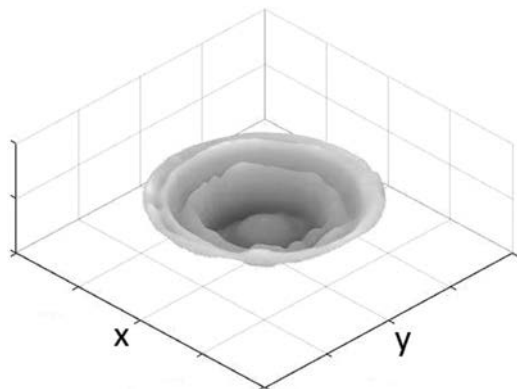


Fig. 19e. 6516 Hz

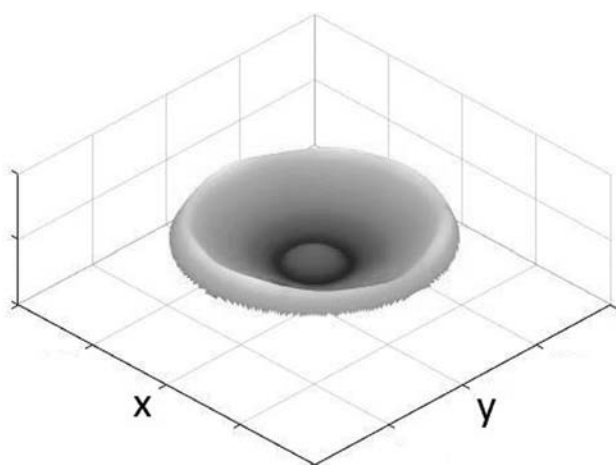


Fig. 19f. "Piston mode"

The investigation of these factors is an important step towards fully understanding the functioning of a loudspeaker and improving its quality.

Along with the correctly-working sample reported in previous sections, we tested multiple samples of loudspeakers built on purpose with deviations from the nominal properties. The defects concerned (1) materials and properties of components and (2) variations of assembling process.

Although we validated the capability of computing SPL curves obtained from the laser vibrometry with good correspondence to those measured with a microphone, here we will focus onto the AAL curve of each sample, as it is a pure vibration measure and less elaborated compared to the SPL.

Fig. 20 illustrates the deviations between all AAL curves of the tested samples of woofers with variations in components and assembling. Studying the response of defective samples we could draw a conclusion about dependency between the behavior of AAL/SPL and a particular defect.

The inverse problem is to spot a defect from the response of the loudspeaker through comparing it with a perfect nominal curve and looking for the similar alignment in the database that we managed to elaborate performing tests on the items with artificially introduced imperfections. However, in practice certain defects can compensate, or vice versa, amplify their effect on the vibration response of the

device and due to this it becomes difficult to precisely identify the cause of imperfections. So the defect identification technique still remains to be improved. And for this, the analysis of the harmonic distortion products looks appealing and will be implemented in the future.

### 3 CONCLUSIONS

The experimental approach introduced in this paper benefits from the synchronized exponential sine sweep excitation technique coupled with an accurate LDV vibration measurement system. In this way, we managed to extract a very "clean" impulse response of the system in hundredths of points, removing most of the noise and ensuring perfect linearity. It appears that this method had not been previously applied to a Doppler Laser Vibrometer (that measures velocity) albeit Klippel already employed it with a triangulation laser (that measures displacement) [14]. The two methods, indeed, are quite different. On one side, a triangulation laser measures all the three coordinates X, Y, Z of each measurement point, providing a real 3D map of the device under test (DUT). In our case, it has been necessary to extrapolate coordinates from a 3D CAD model, which could not be perfectly representative of the DUT. On the other side, due to displacement measure, the output of a triangulation laser has to be differentiated twice to get acceleration, and this operation leads to a worse S/N ratio by high frequencies because for every differentiation there is a decay of 6 dB/oct in the spectrum. As a result, triangulation lasers need to be used with higher voltage for the loudspeaker (and this could bring the DUT out of linear behavior) or in a lower frequency range. Our measurements cover a wide frequency range with optimal S/N ratio and remains within the rated operational range of both DUT and measuring system.

Further numerical elaboration of results permits to convert from the measured acceleration spectra in each point to global estimated acoustical curves of AAL and SPL. This approach allowed getting an insight on the vibrational behavior of a loudspeaker and how it interferes with the acoustic response of the device. The present study shows the advantages of using experimental and numerical tools in combination.

Another merit of laser vibrometer analysis is the possibility to study modes of vibrations at frequencies of strong peak or valleys, to investigate the in-phase and anti-phase components of SPL/AAL, to provide essential data for validation of finite elements simulations, to emulate a video response of a loudspeaker to the sweep excitation, and all this without the usage of an anechoic room. Investigation of how the AAL and SPL curves of a loudspeaker differ from a response considered nominal allows deducing the cause of the deviations, by having measured the effects of several made-on-purpose defects.

This is the first part of the research project and the next part, concerning finite element analysis of loudspeakers and analysis of the not-linear response, will be subject of a future report.

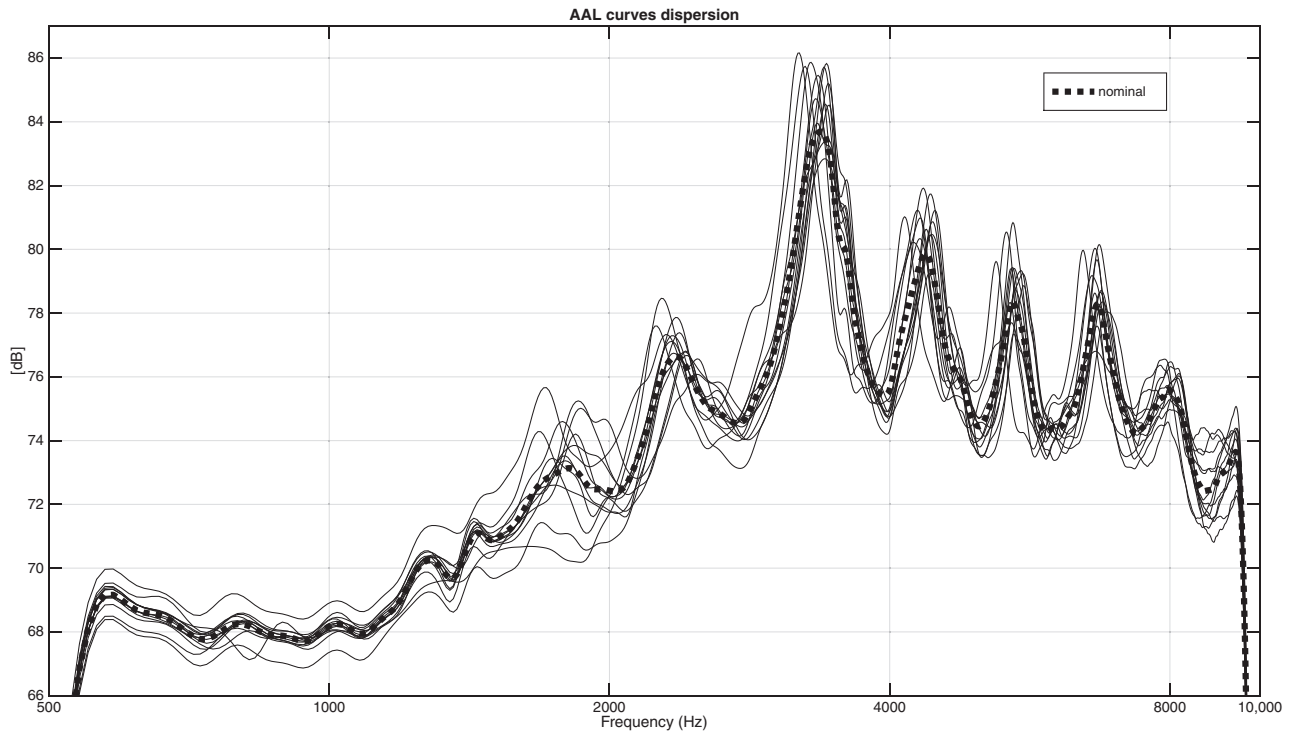


Fig. 20. AAL comparison between all samples measured

#### 4 ACKNOWLEDGMENTS

This research was funded by ASK Industries to which the authors are grateful.

#### 5 REFERENCES

- [1] S. Kinoshita and B. N. Locanthi “The Influence of Parasitic Resonances on Compression Driver Loudspeaker Performance,” presented at the *61st Convention of the Audio Engineering Society* (1978 Nov.), convention paper 1422.
- [2] G. Behler and M. Vorländer “Reciprocal Measurements on Condenser Microphones for Quality Control and Absolute Calibration,” *Acta Acustica united with Acustica*, vol. 90, no.1, pp. 152–160(9) (2004 Jan./Feb.)
- [3] J. N. Moreno “Measurement of Loudspeaker Parameters Using a Laser Velocity Transducer and 2-Channel FFT Analysis,” *J. Audio Eng. Soc.*, vol. 39, pp. 243–249 (1991 Apr.).
- [4] J. Vanherzeele, S. Vanlanduit, and P. Guillaume “Acoustic Source Identification Using a Scanning Laser Doppler Vibrometers,” *Optics and Lasers in Engineering*, vol. 45, pp. 742–749 (2007 Jun.).
- [5] J. Frejlich and P.M. Garcia “Advances in Real-Time Holographic Interferometry for the Measurement of Vibrations and Deformations,” *Optics and Lasers in Engineering*, vol. 32, pp. 515–527 (2000).
- [6] C. Shakher and S. Prakash “Monitoring/Measurement of Out-of-Plane Vibrations Using Shearing Interferometry and Interferometric Grating,” *Optics and Lasers in Engineering*, vol. 38, no. 5, pp. 269–277 (2002).
- [7] S. Prakash, S. Upadhyay, and C. Shakher “Real Time Out-of-Plane Vibration Measurement/Monitoring Using Talbot Interferometry,” *Optics and Lasers in Engineering*, vol. 33, no. 4, pp. 251–259 (2000).
- [8] L. Tronchin “The Emulation of Nonlinear Time-Invariant Audio Systems with Memory by Means of Volterra Series,” *J. Audio Eng. Soc.*, vol. 60, pp. 984–996 (2012 Dec.).
- [9] L. Tronchin and V. L. Coli “Further Investigations in the Emulation of Nonlinear Systems with Volterra Series,” *J. Audio Eng. Soc.*, vol. 63, pp. 671–683 (2015 Sep.).
- [10] A. Farina, “Simultaneous Measurement of Impulse Response and Distortion with a Swept-Sine Technique,” presented at the *108th Convention of the Audio Engineering Society* (2000 Feb.), convention paper 5093.
- [11] W. Klippel and J. Schlechter “Distributed Mechanical Parameters Describing Vibration and Sound Radiation of Loudspeaker Drive Units,” presented at the *125th Convention of the Audio Engineering Society* (2008 Oct.), convention paper 7531.
- [12] J. Schlechter and W. Klippel, “Visualization and Analysis of Loudspeaker Vibrations,” presented at the *121st Convention of the Audio Engineering Society* (2006 Oct.) convention paper 6882.
- [13] A. Novák, L. Simon, F. Kadlec, and P. Lotton “Nonlinear System Identification Using Exponential Swept-Sine Signal,” *IEEE Transactions on Instrumentation and Measurement*, vol. 59, no. 8, pp. 2220–2229 (2010 Aug.)
- [14] A. Farina, “Advancements in Impulse Response Measurements by Sine Sweeps,” presented

at the *122nd Convention of the Audio Engineering Society* (2007 May), convention paper 7121.

[15.] <http://www.aurora-plugins.it/>

[16] E. B. Skrodzka and A. P. Scîek, "Comparison of Modal Parameters of Loudspeakers in Different Working Conditions," *Applied Acoustics*, vol. 60, pp. 267–277 (2000).

## THE AUTHORS



Maria Costanza Bellini



Luca Collini



Angelo Farina



Daniel Pinardi



Kseniia Riabova

Maria Costanza Bellini got a Master Degree in telecommunications engineering at the Polytechnic of Turin in 2014 and she is currently a Ph.D student at the University of Parma, working on experimental and theoretical analysis of the acoustics of loudspeakers. She spends most of her time in the acoustics labs of ASK Industries in Monte San Vito, Ancona, Italy, where she is responsible of the tests in the anechoic room.

Luca Collini is associate professor of machine design at the Department of Engineering and Architecture of the University of Parma since 2014. He graduated with a degree in mechanical engineering in 2000, and got a Ph.D. in industrial engineering in 2005 with a thesis on the micromechanical modelling of heterogeneous materials. He is teacher at the University of Parma in the Faculty of Mechanical and Management Engineering. He is in the Commission for the professional evaluation of engineers, member of the Committee for evaluation of foreign language, member of the Italian Association for Stress Analysis, and member of the Italian Group of Fracture. He spent two research periods abroad, in 2001 at the Department of Materials Science, University of Zilina (Slovakia), and in 2002–2003 at the Institute of Physics of Materials, Academy of Sciences in Brno (Czech Republic), working on the fatigue of metallic materials. He is the author of about 100 scientific publications and articles in journals and proceedings of Italian and international conferences; his research activity focuses on mechanical behavior of materials and NDT techniques.

Angelo Farina got his Master Degree in civil engineering in December 1982 at the University of Bologna, Italy, with a thesis on the acoustics and vibrations inside a tractor cab. In 1987 he got a Ph.D. in technical physics at the University of Bologna with a thesis on experimental assessment of concert hall acoustics. He was a full-time researcher since 1<sup>st</sup> November 1986 at the University

of Bologna, and since 1<sup>st</sup> march 1992 at the University of Parma, where he became Associate Professor on 1<sup>st</sup> November 1998 and Full Professor of environmental applied physics since 1<sup>st</sup> May 2005, where he has the chair of applied acoustics and environmental applied physics. During his academic career Angelo worked in several fields of applied acoustics, including noise and vibration, concert hall acoustics, simulation software and advanced measurement systems. In the last 10 years Angelo focused mostly on applications involving massive microphone and loudspeaker arrays. In 2008 he was awarded with the AES fellowship for his pioneering work on electroacoustic measurements based on exponential sine sweeps. Angelo is author of more than 250 scientific papers and three widely-employed software packages (Ramsete, Aurora Plugins, DISIA).

Daniel Pinardi got a Master Degree in mechanical engineering at the University of Parma, Italy, in July 2016. During his studies met Angelo Farina, who became his supervisor for a vibroacoustic thesis on automotive loudspeakers. Now he is continuing his studies in acoustics as a Ph.D. student and, as a research fellow, is part of a new project about the application of active noise control systems for random noise on automotive vehicles.

Kseniia Riabova got her Master Degree in mechanical engineering at the Kharkiv Polytechnic Institute, Ukraine, in June 2011. After this she made two internships—at RWTH Aachen University, Germany in 2011 and at McGill University, Montreal, Canada, in 2015. She completed her Ph.D. in Industrial Engineering at the University of Parma in March 2017, and she is currently a post-doc research fellow at the Dept. of Engineering and Architecture of the University of Parma, where she is conducting research associated with modelling of material behavior and finite element simulations.